Expression and function of nuclear receptor coregulators in brain: understanding the cell-specific effects of glucocorticoids

Laan, S. van der

Chapter II

Neuroanatomical distribution and colocalisation of nuclear receptor corepressor (N-CoR) and silencing mediator of retinoic and thyroid (SMRT) receptors in rat brain

S van der Laan , SB Lachize, TG Schouten, E Vreugdenhil, ER de Kloet and OC Meijer

Abstract

The two structurally related Nuclear Receptor Corepressor (N-CoR) and Silencing Mediator of Retinoid and Thyroid receptors (SMRT) proteins have been found to differentially affect the transcriptional activity of numerous nuclear receptors, such as thyroid hormone, retinoic acid and steroid receptors. Because of the numerous effects mediated by nuclear receptors in brain, it is of interest to extend these *in vitro* data and to explore the cellular distribution of both corepressors in brain tissue. We therefore examined, using *in situ* hybridisation, whether the relative abundance of these two functionally distinct corepressors differed in rat brain and pituitary. We find that although both N-CoR and SMRT transcripts are ubiquitously expressed in brain, striking differences in their respective levels of expression could be observed in discrete areas of brain stem, thalamus, hypothalamus and hippocampus. Using dual-label immunofluorescence, we examined in selected glucocorticoid sensitive areas involved in the regulation of the hypothalamus-pituitary-adrenal axis activity, the respective protein abundance of N-CoR and SMRT. Protein abundance was largely concurrent with the mRNA expression levels, with SMRT relatively more abundant in hypothalamus and brain stem areas. Colocalisation of N-CoR and SMRT was demonstrated by confocal microscopy in most areas studied. Taken together, these findings are consistent with the idea that the uneven neuroanatomical distribution of N-CoR and SMRT protein may contribute to the site-specific effects exerted by hormones, such as glucocorticoids, in the brain.

1. Introduction

Nuclear receptors are ligand-inducible transcription factors that modulate gene expression by specifically binding to responsive elements in promoter regions of target genes. The nuclear receptor family consists of type I receptors (e.g. estrogen, progesterone, androgen, mineralocorticoid and glucocorticoid receptors (ER, PR, AR, MR and GR)), type II receptors (e.g. retinoic acid, thyroid hormone and vitamin D receptors (RAR, TR and VDR)) and orphan receptors (1). These receptors are widely distributed in an uneven manner over many brain regions. The neuroanatomical distribution of the receptors does not satisfactorily explain site-specific effects elicited by their cognate ligand. Previously we have reported an uneven distribution for the two splice variants of the most abundantly expressed p160 coactivator in the rodent brain that have distinct effects on for example the GR and MR (2,3).

Two structurally related but functionally distinct proteins, Silencing Mediator of the Retinoid and Thyroid receptor (SMRT) and Nuclear Corepressors (N-CoR) have both emerged as key players in the mechanism of nuclear receptor mediated gene repression (4,5). N-CoR and SMRT repress gene expression by binding directly to the nuclear receptor and facilitating the recruitment of chromatin remodelling enzymes. They are well-documented, structurally-related corepressor proteins of approximately 270 kDa, which repress gene transcription by recruiting histone deacetylases to the proximity of the nuclear receptor and forming corepressor complexes (6).

While both corepressors originally were defined as repressors of type II nuclear receptors, such as thyroid hormone receptor (TR) and retinoic acid receptor (RAR), they have now been shown to alter the transcriptional activity of steroid receptors *in vitro* (7-9). For example, the dose-response curve of agonist-activated GR and MR is shifted to the right in presence of corepressor proteins. This was observed for endogenous as well as for synthetic ligands (10). Consequently, it has been proposed that at sub-saturating levels of steroids, the presence of corepressor proteins will influence the genomic effects of the ligand-activated nuclear receptors. Although N-CoR and SMRT share structural similarities, it is noteworthy that they have been shown to differentially affect nuclear receptor signalling (8). Therefore, we hypothesise that their relative abundance might determine the effects of steroids on gene transcription. Because of the numerous effects mediated by nuclear receptors in brain, it is of interest to extend these *in vitro* data and to explore the cellular distribution of both corepressors in brain tissues.

We mapped the expression and the relative abundance of N-CoR and SMRT mRNA in rat brain and pituitary gland. Our particular interests are the site-specific effects elicited by glucocorticoid hormones in the brain (for review (11)) and the regulation of the hypothalamus-pituitary-adrenal axis (HPA-axis). Therefore, we demonstrated the respective levels of expression on protein level by means of immunofluorescence in GR and/or MR expressing areas that are important in the regulation of the HPA-axis activity.

2 Material & Methods

2.1 Animals and tissue preparation

Adult male Wistar rats (240g; n=8) were obtained from Charles River Laboratories (Germany). All animals were group-housed (n= 4 per cage) had *ad libitum* access to food and water, and were maintained under controlled conditions, on a 12:12 hour light cycle (lights on from 08.00 to 20.00 h). One week after arrival, all rats were sacrificed in the morning (between 9:00 and 11:00 a.m.). The brains were snap frozen in isopentane (cooled in an ethanol-dry ice

bath) and the pituitaries were frozen on dry ice. All tissues were stored at -80°C until further use. Experiments were carried out with the approval of the Animal Care Committee of the Faculty of Medicine, Leiden University, The Netherlands (DEC nr. 03130).

2.2 In situ hybridisation

Brains of male Wistar rats were used for the *in situ* hybridization procedure (n=4). Thin sections of both brains (20µm) and pituitaries (10 µm) were cut on a cryostat (Leica CM3050S), thaw-mounted on poly-L-lysine (Sigma) coated slices, and stored at -80°C. The sections were fixed for 30 min. in freshly made 4% para-formaldehyde (Sigma) in phosphate buffered saline (PBS, pH 7.4), rinsed twice in PBS, acetylated in triethanolamine (0.1 M, pH 8.0) with 0.25% acetic anhydride for 10 min, rinsed for 10 min in 2 x SSC (SSC: 150 mM sodium chloride, 15 mM sodium citrate), dehydrated in an ethanol series, air dried and stored at room temperature until the *in situ* hybridisation. N-CoR and SMRT riboprobes were amplified by PCR on genomic DNA. For N-CoR, a segment of 482 nucleotides (Genbank Accession number U35312; nucleotide 4715 to 4654) and for SMRT, a segment of 381 nucleotides (Genbank Accession number AF113001; nucleotide 7217 to 7597), was inserted in a PGEMT-easy vector. These murine fragments contained minimal cross-homology and showed 96% identity with corresponding rat mRNA. Hybridisation mix consisted of 50% formamide, 20% dextran sulfate, 1.2 mM EDTA (pH 8.0), 25 mM sodium phosphate (pH 7.0), 350 mM sodium chloride, 100 mM DTT and, 1% Denhardt's, 2% RNA-DNA mix, 0.2% nathiosulfate and 0.2% sodium dodecyl sulfate. A 100 µl aliquot of hybridisation mix containing 2.5 x 10^6 dpm of N-CoR or SMRT riboprobe was added to each section. Coverslips were brought on the slides which were hybridised overnight in a moist chamber at 55°C. The next morning, coverslips were removed and the sections washed in graded salt/formamide at optimised temperature. After the washing steps, sections were dehydrated in a series of ethanol baths and air dried.

The N-CoR and SMRT hybridised sections were apposed to Kodak BioMax MR film for 13 and 7 days, respectively. After development of the films the sections were counter-stained with 0.5% cresyl violet for anatomical analysis. Control sections were treated identically to experimental sections except that sense riboprobes were used. Control sections did not give signal above background.

2.3 Immunofluorescence and confocal laser scanning microscopy

Brains of adult male Wistar rats were used for the immunohistochemistry experiments (n=4). Thin brain sections (20µm) were cut on a cryostat (Leica CM3050S), thaw-mounted on poly-L-lysine (Sigma) coated slices, and stored at -80°C until further use. Slides were allowed to thaw at 4°C during 20 min. prior to fixation. The sections were fixed during 10 min. in pre-chilled methanol/acetone/water [40:40:20 (v/v/v)] solution at 4°C. After fixation, sections were washed three times in 1x phosphate-buffer saline with 0.2% Tween (1 x PBST pH 7.4) and blocked 60 min in 5% normal donkey serum (NDS) at room temperature. Incubations with anti-N-CoR (Santa Cruz biotechnologies; goat polyclonal C-20, 1:50) and anti-SMRT (Upstate; rabbit polycolonal cat. # 06-891, 1:200) primary antibodies were performed overnight at 4°C. The next morning, the sections were allowed to acclimatise for one hour to room temperature, washed three times in 1 x PBST. Detection of N-CoR and SMRT positive cells was realized with FITC conjugated donkey-anti-goat IgG (Santa Cruz biotechnologies; sc-2024, 1:50) and Cy3 conjugated donkey-anti-rabbit IgG (Upstate; 1:150), respectively. Sections were incubated with the secondary antibodies for 60 min. at 37°C. After incubation, sections were washed in 1 x PBST and counter-stained for 10 min. with Hoechst 33528, and washed four times (5 min.) in 1 x PBST. All sections were embedded in polyaquamount

(Polysciences, inc.) and observed with an immunofluorescence microscope (Leica DM6000) or a confocal laser scanning microscope (Bio-Rad Radiance 2100MP). Control sections were incubated with equal amounts of non-immune rabbit and goat sera, which were used as substitute for the primary antibodies. Nuclear immunoreactivity was used for quantification. The amount of non-specific nuclear immunoreactivity was found to vary for each brain area studied and consequently was deducted from the total signal obtained within the corresponding area. For confocal microscopy, Bio-Rad Radiance apparatus equipped with a HeNe and Argon laser was used and the image analysis was performed with a Kalman collection filter (2 scans).

2.4 Analysis and Quantification

For analysis of the relative optical density (ROD) for *in situ* hybridisation and the immunofluorescence, ImageJ 1.32j software (NIH, USA) was used. The mRNA expression was measured for four rats, guided by cresyl-violet counterstained sections and a rat brain atlas (12). The autoradiographs were scanned (1000 dpi) and saved as uncompressed 8-bit grey-scale tiff files. Images of adjacent sections hybridised with N-CoR and SMRT riboprobes were opened in ImageJ to allow visual comparison during analysis. Signal was obtained by subtracting the sense signal from the anti-sense signal. To allow brain wide comparison of expression levels for each transcript, signals were normalized for each rat against the darkest signal (the granular cell layer of the dentate gyrus (DG) in both cases) as previously described (2). The average expression level per area was then assigned to a category according to the percentile of their grey values: +/- < 25%; + 25-35 %; ++ 35-60 %, +++ 60-90 %; ++++ > 90%. Measures for relative abundance of the two transcripts was obtained by dividing the mean relative optical densities (ROD) measured for N-CoR by the mean ROD measured for SMRT for the selected glucocorticoid sensitive areas.

For the evaluation of the immunofluorescent signal a more limited number of brain regions were evaluated for practical reasons. Images were captured and saved as uncompressed tiff files. Per brain region, the collected images for N-CoR (green), SMRT (red) and the Hoechst staining (blue) were merged. Guided by the Hoechst-stain, nuclear optical density was measured. Immunoreactivity of multiple individual cells was measured per brain region. Non-specific signal (non-immune sera) was measured for each region and subtracted from the total signal to obtain the specific signal. An equal amount of cell nuclei were measured per region per rat. Differences between brain areas in corepressor stoichiometry were determined by taking the ratio of N-CoR and SMRT immunoreactive signal for specific glucocorticoid sensitive areas.

2.5 Statistics

One-tailed non-parametric Wilcoxon Signed Rank Test was used to statistically assess differences in the relative protein abundance, as it could be predicted from the mRNA mapping. Differences were considered significant at $p < 0.05$.

3. Results

3.1 N-CoR and SMRT mRNA expression in brain

N-CoR and SMRT transcripts were ubiquitously detected in brain tissue. Representative SMRT hybridisation autoradiographs (fig.1) and semi-quantification of the signal intensity are summarised in table 1.

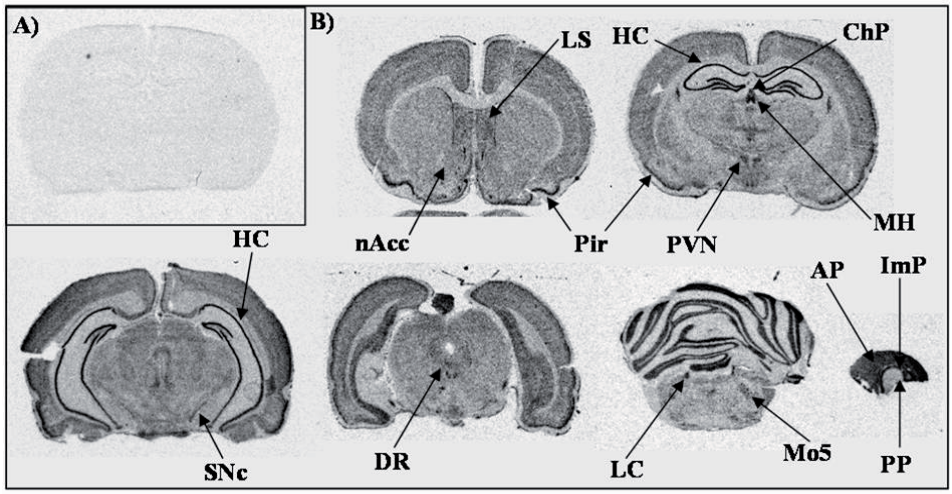

Fig.1 Specificity of hybridisation with 35S labelled sense riboprobe (A). Expression of SMRT mRNA in a series of coronal sections of the rat brain (B). LS, lateral septum; HC, hippocampus; ChP, choroid plexus; Pir, piriform cortex; PVN, paraventricular nucleus of the hypothalamus; MH, medial habenula; SNc, substantia nigra, compact part; DR, dorsal raphe; LC, locus coeruleus; Mo5, motor trigeminal nucleus; AP, anterior pituitary; PP, posterior pituitary; ImP, intermediate lobe; nAcc, nucleus accumbens core.

Although we found overlapping pattern of distribution for both N-CoR and SMRT, clear differences in their relative transcript abundance were observed in several brain regions (fig.2). The anterior pituitary showed a homogenously distributed signal of both SMRT and N-CoR (fig.1).N-CoR hybridisation signal was high in the hippocampus (60-90%) with the granular cell layer of the DG exhibiting the strongest signal (set at 100%). The overall N-CoR anti-sense hybridisation level was markedly higher in the thalamus (35-60%) than in the hypothalamus (25-35%). Cortical areas and the cerebellar lobules showed high, homogenously distributed, hybridisation signals (60-90%). Brain stem nuclei signals, such as for the locus coeruleus and the oculomotor nucleus, hardly exceeded background levels (<25%) (fig.2).

SMRT hybridisation signal was very high in all hippocampal subregions (CA1-CA3 >90%). Cortical areas and cerebellar lobules exhibited homogenous moderate (35-60%) and high SMRT hybridisation degrees (60-90%), respectively. Hypothalamic nuclei, such as the suprachiasmatic and the supraoptic nucleus of the hypothalamus, clearly showed very high levels of SMRT hybridisation (>90%). Most motor nuclei studied, among which the substantia nigra compact part (SNc), the oculomotor and facial nucleus, showed high levels of SMRT hybridisation (60-90%). The hybridisation signal for SMRT in the thalamus was low to moderate (25-60%). Brain stem nuclei such as the locus coeruleus (LC), exhibited high signal (60-90%). As *in situ* hybridisation is a semi-quantitative technique, N-CoR and SMRT levels of expression can not be compared in one brain area.

	N-CoR	SMRT		N-CoR	SMRT
CORTICAL AREAS			HYPOTHALAMUS		
Frontal cortex, area 2	+++	++	Suprachiasmatic nucleus	++	++++
Tenia tecta	++	++	Supraoptic nucleus	++	++++
Olfactory tubercle	+++	+++	Paraventricular nucleus of the hypothalamus		
Piriform cortex	+++	++++	magnocellular part	+	+++
			parvocellular part	+	+++
HIPPOCAMPUS			Ventromedial hypothalamic nucleus	++	+++
Dentate gyrus = 100%			Arcuate hypothalamic nucleus	+++	+++
Hippocampus CA3 – pyramidal layer	+++	++++	Anterior hypothalamic area	+	++
Hippocampus CA2 – pyramidal layer	+++	++++	Posterior hypothalamic nucleus	++	++
Hippocampus CA1 – pyramidal layer	+++	++++	Supramammillary nucleus	++	+++
			Medial supramammillary nucleus	++	+++
AMYGDALA COMPLEX					
Dorsal endopiriform nucleus	++	++	MOTOR		
central amygdaloid nucleus	++	++	Oculomotor nucleus	+	+++
Lateral amygdaloid nucleus	++	++	Facial nucleus	+/-	+++
			Substantia nigra, reticular part	+/-	+
SEPTAL COMPLEX			Substantia nigra, compact part	++	+++
Septohippocampal nucleus	++	+++	Motor trigmenial nucleus	+	+++
Lateral septal nucleus, ventral	+	++	RETICULAR CORE		
Lateral septal nucleus, dorsal	+	++	Dorsal raphe nucleus	++	++
Bed nucleus of the stria terminalis,	++	++	Locus coeruleus	+/-	+++
medial division, posterointermediate part			Pontine nuclei	+	++
			Pontine reticular nucleus, oral part	+/-	+
BASAL GANGLIA					
Caudate putamen	++	++	BRAINSTEM SENSORY		
Accumbens nucleus, core	++	++	Mesencephalic trigeminal nucleus	+	+++
Globus pallidus	+/-	+			
			PRE-& POSTCEREBELLAR NUCLEI		
THALAMUS			Red nucleus	+	+++
Paraventricular thalamic nucleus	+++	+++			
Paratenial thalamic nucleus	++	++	Choroid plexus	++	++
Reticular thalamic nucleus	++	++	Cerebellar lobule 2	+++	+++
Zona incerta	++	++			
Medial habenular nucleus	+++	+++	PITUITARY		
Ventrolateral thalamic nucleus	++	+	Anterior pituitary	+++	++++
Ventral lateral geniculate nucleus,			Intermediate lobe	+++	++++
magnocellular part	++	+	Posterior pituitary	+/-	+/-

tabel 1. Regional expression of N-CoR and SMRT mRNA in the rat brain and pituitary. Prior to the calculation of the mean (n= 4), the signal was normalised per rat against the highest in situ hybridisation signal, i.e. the signal of the granular cell layer of the DG in all cases. Signal in the DG was set at 100% (scale is % of DG signal: +/- < 25%; + 25-35 %; ++ 35-60 %, +++ 60-90 %; ++++ > 90%).

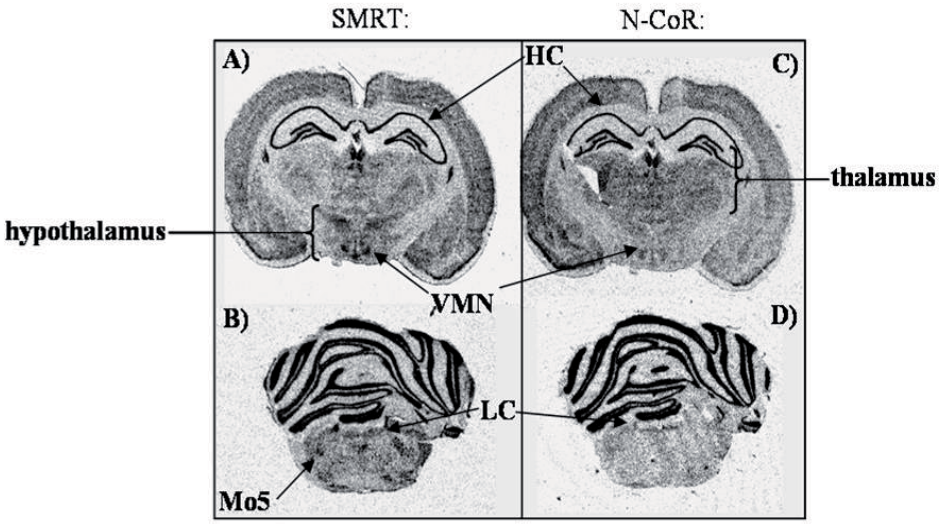

Fig. 2 Adjacent sections of SMRT (A and B) and N-CoR (C and D). SMRT and N-CoR show substantial differences in their respective levels of mRNA abundance in certain brain areas. The most striking differences are high levels of SMRT expression in hypothalamus and brain stem and high N-CoR expression in thalamus. HC, hippocampus; VMN, ventromedial nucleus; LC, locus coeruleus; Mo5, motor trigeminal nucleus.

In line with our working hypothesis that the modulation of gene transcription by glucocorticoids is dependent on the type and amount of corepressor present, we calculated the relative abundance of the corepressors by dividing the mean relative optical densities measured for N-CoR by the mean relative optical densities measured for SMRT in a number of selected glucocorticoid sensitive areas, *i.e.* hippocampal subfields, the hypothalamic paraventricular nucleus (PVN), the serotonergic dorsal raphe nucleus (DR), and the noradrenergic locus coeruleus (table 2).

Brain area	N-CoR/SMRT
CA3	0.63 ± 0.05
DG	**0.77 ± 0.06**
PVNp	0.64 ± 0.01
DR	0.61 ± 0.06
LC	**0.33 ± 0.04**

Table 2. Relative transcript abundance (± sem). The ROD of the signal obtained for N-CoR was divided by the ROD obtained for SMRT in 5 selected glucocorticoid sensitive areas. The LC has the lowest ratio of the areas studied indicating that it is a SMRT-enriched brain region.

This has two major advantages: 1) it corrects for the inherent differences in signal intensity observed between brain nuclei due to varying cell densities and 2) generates an adequate value for comparison of the relative abundance of both transcripts in different areas. The data show that the dentate gyrus is, relatively to the other areas studied, enriched in N-CoR mRNA, while the LC is SMRT-enriched; reflecting the overall hardly detectable N-CoR signals in brain stem nuclei (fig. 2).

3.2 N-CoR and SMRT protein expression in brain

The distribution of cells double-labeled for N-CoR and SMRT was in all areas studied in line with their respective levels found on mRNA. Representative pictures are shown in fig 3. Interestingly, specific cytoplasmic staining for N-CoR, but not SMRT, was observed in pyramidal cells in cortical areas and hippocampus (fig. 3b). This signal was observed but not quantified. Measurement of the nuclear immunoreactivity signal is summarised for N-CoR and SMRT in fig. 4a and fig. 4b, respectively.

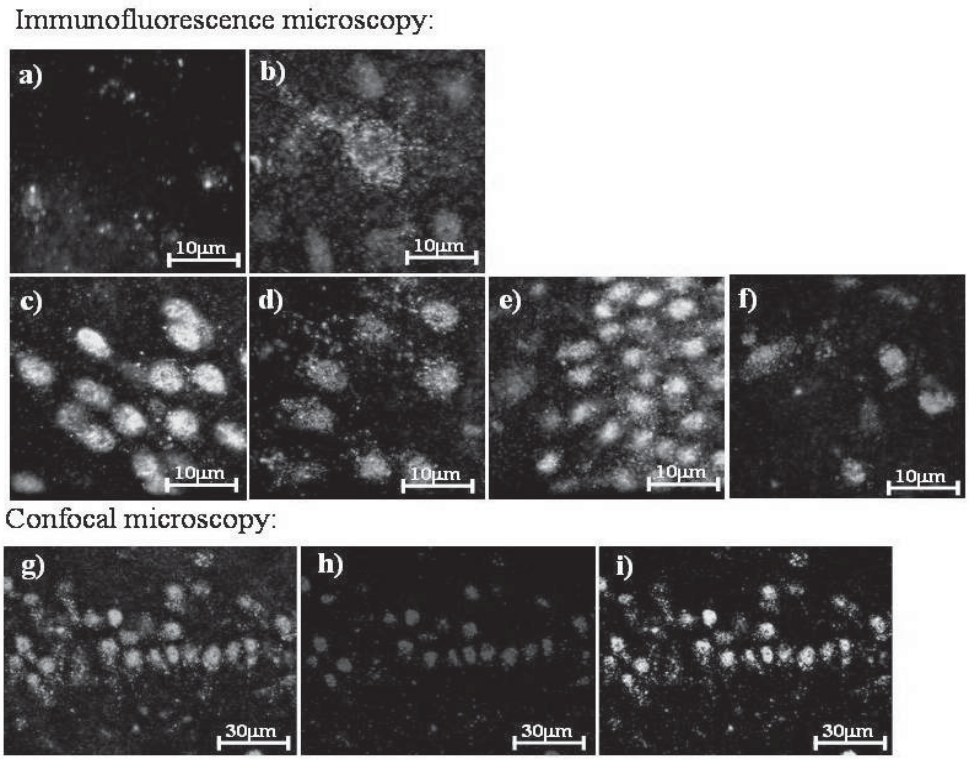

Fig. 3 Dual-immunofluorescence images for N-CoR and SMRT. The merged images show N-CoR (FITC:green) and SMRT (Cy3:red). A: Control IgG image of the aspecific immunoreactivity of non-immune sera. B: Cytoplasmic expression of N-CoR is observed in the pyramidal neurons of the frontal cortex. C-F: Relative expression of N-CoR and SMRT differs in the piriform cortex (c), CA3 (d), dentate gyrus (e) and the locus coeruleus (f). G-I: Confocal microscopy image of N-CoR (g) and SMRT (h) in the nucleus of the CA1 neurons. Colocalisation of the corepressors is shown in yellow (i). (see colour image page 123).

In general the distribution of N-CoR immunoreactivity (N-CoR-ir) paralleled that of its mRNA expression. N-CoR protein was predominantly detected in regions of the forebrain while N-CoR-ir hardly exceeded background levels in brain stem nuclei such as the LC (fig. 4a). In the hypothalamus, N-CoR-ir was higher then expected based on the signal measured by *in situ* hybridisation (fig. 2c). N-CoR-ir was only moderate in all hippocampal subregions, but high in another cell-dense area, the piriform cortex (Pir). Nevertheless, the relative N-CoR-ir within the subregions of the hippocampus paralleled the mRNA expression with the cells of the DG showing a higher N-CoR-ir than the CA3 (table 1). N-CoR-ir was similar in the cells of the DR and the parvocellular part of the paraventricular nucleus (PVNp).

SMRT protein distribution also matched the expression pattern observed for *in situ* hybridisation. SMRT immunoreactivity (SMRT-ir) was clearly discernible in hypothalamus, brain stem, and to a lesser extent, in the subregions of the hippocampus (fig 4b). In a similar manner as for N-CoR-ir, SMRT-ir was high in the Pir and moderate in the subregions of the hippocampus. Again, SMRT-ir within the subregions of the hippocampus matched the mRNA distribution; with the cells of the CA3 exhibiting the highest immunoreactivity. The highest SMRT-ir was observed in the magnocellular part of the paraventricular nucleus (PVNm). SMRT-ir in the PVNp and the DR was found to be comparable indicating that both regions do not significantly differ in their SMRT content. In contrast, SMRT-ir was approximately 1.5 times higher in the LC than in the DR.

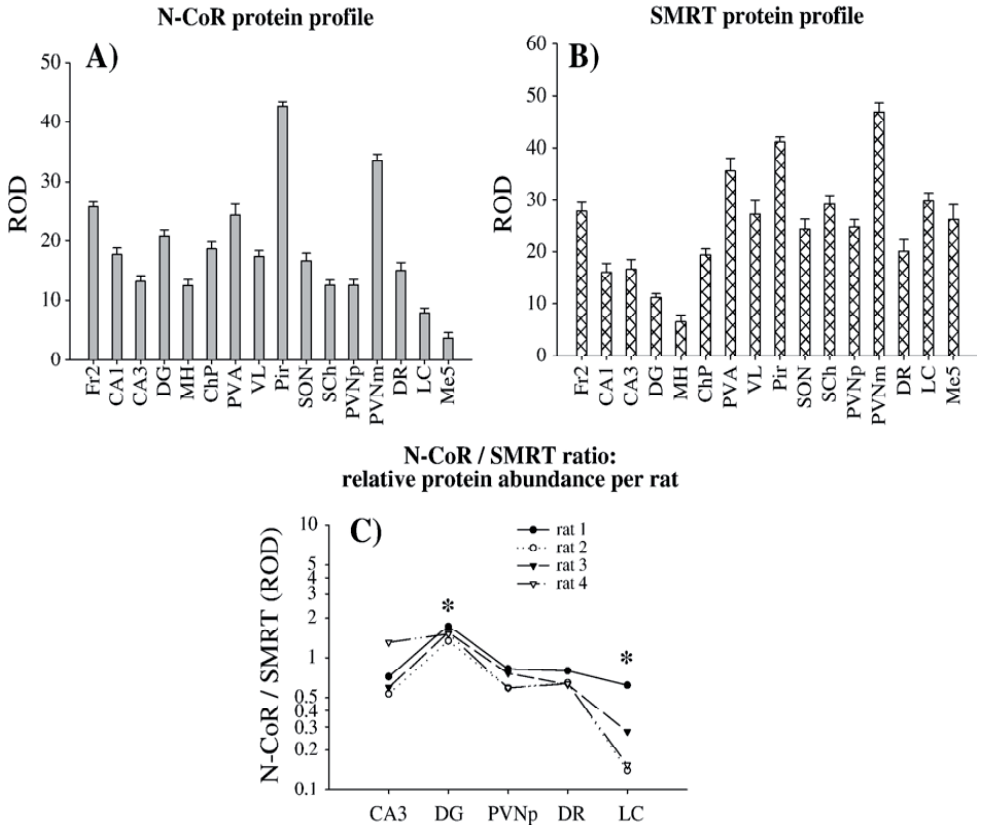

Fig. 4 N-CoR and SMRT protein expression in different areas. A,B: N-CoR (A) and SMRT (B) immunoreactivity as mean relative optical density (ROD) and standard error of the mean. Fr2, frontal cortex area 2; CA1 and CA3, hippocampus CA1 and CA3-pyramidal layer; DG, dentate gyrus; MH, medial habenula; ChP, choroid plexus; PVA, paraventricular thalamic nucleus; VL, ventrolateral thalamic nucleus; Pir, piriform cortex; SON, supraoptic nucleus; SCh, suprachiasmatic nucleus; PVNp, paraventricular hypothalamic nucleus, parvocellular part; PVNm, paraventricular hypothalamic nucleus, magnocellular part; DR, dorsal raphe nucleus; LC, locus coeruleus; Me5, mesencephalic trigeminal nucleus.C: N-CoR/SMRT ratio in selected glucocorticoid areas in individual rats (n= 4). The order of the brain nuclei is arbitrary and the lines drawn in-between is for visualisation purposes only. Asterisks indicate significantly different ratios compared to all other regions.

To compare the respective levels of nuclear N-CoR and SMRT protein, we calculated (in a similar manner as described for the relative mRNA expression analysis) the relative immunoreactivity in 5 selected glucocorticoid and/or mineralocorticoid receptor expressing

brain regions involved in the regulation of the HPA axis (fig. 4c). The ratios of N-CoR/SMRT follow the same pattern for each individual rat. The DG is a significantly N-CoR-enriched brain region compared to the other areas studied (NCoR/SMRT ratios approaching 1.5). Similarly, the LC is significantly SMRT-enriched brain region. The CA3, PVNp and DR cells did not significantly differ in their relative N-CoR and SMRT nuclear protein abundance (ratios approximately 0.8).

3.3 Nuclear distribution of N-CoR and SMRT

Colocalisation of both corepressor proteins within the nucleus was demonstrated by confocal microscopy. Representative pictures of N-CoR and SMRT colocalisation in CA1 hippocampal neurons are shown in fig. 3g-i. The quantification of the nuclear N-CoR-ir and SMRT-ir of all areas studied was performed using immunofluorescence microscopy, i.e. whole cell nuclear signal. Merged confocal picture of N-CoR-ir (green) and SMRT-ir (red) is shown (fig. 3i). The yellow coloring indicates that both proteins colocalise in the CA1 neurons. In general, we found that N-CoR and SMRT proteins colocalise in all areas studied (e.g. hippocampus, PVN, DR, LC) and that their nuclear distribution was speckled. Although N-CoR and SMRT were shown to colocalise in the nucleus of all the cells, nuclear agglomerates containing exclusively N-CoR or SMRT were also observed (data not shown).

4. Discussion

In the present study we examined the neuroanatomical distribution of two functionally distinct corepressors involved in the regulation of gene expression by nuclear receptors. N-CoR and SMRT mRNAs were found to be ubiquitously expressed in brain tissue of young adult male rats. Brain areas such as the cortex, caudate putamen and nucleus accumbens, displayed similar respective levels of expression of both mRNAs. Distinct differences in relative expression were found in discrete regions of the hippocampus, hypothalamus, thalamus and brainstem. We validated this uneven distribution found for both mRNAs at the protein level in glucocorticoid sensitive brain areas that are involved in the regulation of stress-induced HPA-axis activity, i.e. hippocampus, PVN and LC. Furthermore, specific cytoplasmic N-CoR staining was detected in pyramidal cells of cortical areas and the hippocampus. Our results by confocal microscopy indicated that N-CoR and SMRT colocalise *in vivo*, possibly reflecting complexes identified *in vitro* by biochemical purification from HeLa nuclear extracts (13). However, a difference in nuclear distribution of the corepressor proteins (data not shown) was also observed, indicating that even if both proteins associate in homologous complexes, they also are expected to be exclusively present in other nuclear complexes. Taken together, these data reinforce the concept that the uneven distribution of coregulator proteins such as N-CoR and SMRT may have implications for the modulation of site-specific effects of nuclear receptors in brain tissue.

So far, N-CoR and SMRT mRNA expression in rodent brain has primarily been studied in relation to thyroid hormone in juvenile animals (14,15). In an elegant paper, Becker *et al.* also reported an uneven distribution on N-CoR and SMRT mRNA in the hypothalamus of 22 days old mice. Furthermore, in line with our findings, at postnatal day 1, N-CoR transcript was reported to be expressed at high levels in thalamus while SMRT transcript was abundant in the PVN. The parallel expression of N-CoR and SRC1 was also characterised in the fetal and neonatal developing rat brain (14).

While the corepressors have been studied almost exclusively in relation to nuclear processes, we observed cytoplasmic expression of N-CoR in the cortical areas and hippocampus.

Previously, Boutell *et al* convincingly demonstrated using the same antibody as used in our experiments, cytoplasmic localisation of N-CoR in healthy and diseased human brains (16). These authors reported that N-CoR specifically binds to the rat and human Huntington gene product. Although the functional relevance of this interaction remains elusive, these findings and the data in the present study, suggest an additional role of this corepressor protein, apart from its function in nuclear receptor signalling.

The uneven distribution of N-CoR and SMRT suggests distinct physiological roles for both proteins. Assessment of their function on gene transcription was performed in numerous *in vitro* studies. Ligand-activated thyroid hormone receptors transcriptional activity on a well-characterised negative hormone responsive element, showed that SMRT but not N-CoR surprisingly functioned as a coactivator of gene transcription (17). Although Berghagen *et al.* concluded that the hormone response element architecture was important for the function of the corepressor (SMRT), the type of ligand and the amount of corepressor (N-CoR) cotransfected was also found to differentially affect the transcriptional activity of the androgen receptor in CHO cells (18). Additional support for distinct biological roles for N-CoR and SMRT comes from the N-CoR knockout mice which die before birth, indicating that SMRT can not compensate for the lack of N-CoR. Furthermore, the knockout phenotype underlined the importance of N-CoR for at least the development of the nervous system (19).

In our particular interest are the effects elicited by glucocorticoid hormones in the brain. Glucocorticoids bind to two corticosteroid receptors that are widely expressed in the brain, and N-CoR and SMRT expression is high in many areas known to contain MR and/or GR (20-22). In the cells expressing both receptor types, mainly in limbic areas, the MRs and the GRs act in synergism or antagonism on gene transcription, depending on cellular context (23,24). The relative abundance of MR and GR in a cell is a crucial component for the type of effects on gene transcription elicited by the glucocorticoids. However, differences in MR and GR neuroanatomical distribution do not satisfactorily explain cell-specific effects elicited by glucocorticoids on several target genes (corticotrophin releasing factor, phenylethanolamine N-methyltransferase, tyrosine hydroxylase) (25,26).

Our finding that the LC and the substantia nigra differ in their relative N-CoR and SMRT mRNA abundance may be of relevance. The LC was found to be a SMRT-enriched brain area whereas the substantia nigra (SN) expresses both transcripts (see table 1). It is known that chronic cold exposure significantly reduces mRNA expression of the tyrosine hydroxylase (TH) gene (27), the rate-limiting catecholamine biosynthesising enzyme, in the LC whereas it does not affect TH expression in the SN (28,29). In addition, a functional glucocorticoid responsive element has been identified in the 5' flanking promoter region of the TH gene, suggesting that the effects are mediated through DNA-binding of the GR in the promoter region (30,31). Our finding of an uneven expression of N-CoR and SMRT mRNA in brain areas such as in the LC and the SN might in part account for the cell-specific effects of glucocorticoids on TH gene regulation. In the suprachiasmatic nucleus, where no detectable amounts of corticosteroid receptors are expressed, both N-CoR and SMRT are detected (see table 1) indicating that these corepressors are functionally not restricted to the modulation of the transcriptional activity of the corticosteroid receptors.

This uneven distribution of the expression observed for N-CoR (the most striking difference with SMRT has been observed in the brain stem where hardly any detectable amounts were found) may originate from the initial patterning of the central nervous system. Mechanisms such as 'early neural patterning' or 'neural induction' are involved in the subdivision of the neural plate into distinct territories: forebrain, midbrain, hindbrain and spinal cord (for review

(32)). Possibly, this could account for the regional expression of N-CoR reported in our study. Interestingly, the neuroanatomical distribution reported for the coactivators SRC1a and SRC1e by Meijer et al. (2) supply additional support for the proposed explanation, although the expression of the splice variants is presumably governed by a more complex set of genes. Therefore, we speculate that major brain subdivisions might differ in their steroid sensitivity due to a differential expression of transcription coregulators such as N-CoR, SMRT, SRC1a and SRC1e.

The concept that the relative abundance of coregulators in vicinity of promoter regions contributes to cell-specific responses on gene transcription is based on *in vitro* studies. Therefore, the differential distribution of coregulator proteins still has to be examined for its biological relevance. We propose that presented data in combination with the steroid receptor coactivator mapping may offer an explanation and possibly a prediction of the nature of the steroid receptors mediated effects on gene transcription.

5. Acknowledgments

This study was supported by NWO VIDI Grant 016.036.381 (O.C.M.) and the Royal Netherlands Academy for Arts and Sciences (E.R.d.K.). We thank H. de Bont and P.J. Steenbergen for technical support, T.F. Dijkmans for fruitful discussions and Dr. D.L. Champagne for critical reading of the manuscript.

Reference List

1. **Beato M, Herrlich P, Schutz G**. Steroid hormone receptors: many actors in search of a plot *Cell* 1995; 83: 851-857.

2. **Meijer OC, Steenbergen PJ, de Kloet ER**. Differential expression and regional distribution of steroid receptor coactivators SRC-1 and SRC-2 in brain and pituitary *Endocrinology* 2000; 141: 2192-2199.

3. **Meijer OC, Kalkhoven E, van der Laan S., Steenbergen PJ, Houtman SH, Dijkmans TF, Pearce D, de Kloet ER**. Steroid receptor coactivator-1 splice variants differentially affect corticosteroid receptor signaling *Endocrinology* 2005; 146: 1438-1448.

4. **Nagy L, Kao HY, Chakravarti D, Lin RJ, Hassig CA, Ayer DE, Schreiber SL, Evans RM**. Nuclear receptor repression mediated by a complex containing SMRT, mSin3A, and histone deacetylase *Cell* 1997; 89: 373-380.

5. **Jepsen K, Rosenfeld MG**. Biological roles and mechanistic actions of co-repressor complexes *J Cell Sci* 2002; 115: 689-698.

6. **Davie JK, Dent SYR**. Histone modifications in corepressor functions *Current Topics in Developmental Biology, Vol 59* 2004; 59: 145-163.

7. **Ki SH, Cho IJ, Choi DW, Kim SG**. Glucocorticoid Receptor (GR)-Associated SMRT Binding to C/EBP{beta} TAD and Nrf2 Neh4/5: Role of SMRT Recruited to GR in GSTA2 Gene Repression *Mol Cell Biol* 2005; 25: 4150-4165.

8. **Wang Q, Blackford JA, Jr., Song LN, Huang Y, Cho S, Simons SS, Jr**. Equilibrium interactions of corepressors and coactivators with agonist and antagonist complexes of glucocorticoid receptors *Mol Endocrinol* 2004; 18: 1376-1395.

9. **Wang Q, Anzick S, Richter WF, Meltzer P, Simons SS**. Modulation of transcriptional sensitivity of mineralocorticoid and estrogen receptors *Journal of Steroid Biochemistry and Molecular Biology* 2004; 91: 197-210.

10. **Szapary D, Huang Y, Simons SS**. Opposing effects of corepressor and coactivators in determining the dose-response curve of agonists, and residual agonist activity of antagonists, for glucocorticoid receptor-regulated gene expression *Molecular Endocrinology* 1999; 13: 2108-2121.

11. **de Kloet ER, Joels M, Holsboer F**. Stress and the brain: from adaptation to disease *Nat Rev Neurosci* 2005; 6: 463-475.

12. **Paxinos G, Watson C**. *The Rat Brain Atlas in Stereotactic Coordinates*. Academic Press Inc., San Diego, 1996.

13. **Yoon HG, Chan DW, Huang ZQ, Li JW, Fondell JD, Qin J, Wong JM**. Purification and functional characterization of the human N-CoR complex: the roles of HDAC3, TBL1 and TBLR1 *Embo Journal* 2003; 22: 1336-1346.

14. **Iannacone EA, Yan AW, Gauger KJ, Dowling AL, Zoeller RT**. Thyroid hormone exerts site-specific effects on SRC-1 and NCoR expression selectively in the neonatal rat brain *Mol Cell Endocrinol* 2002; 186: 49-59.

15. **Becker N, Seugnet I, Guissouma H, Dupre SM, Demeneix BA**. Nuclear corepressor and silencing mediator of retinoic and thyroid hormone receptors corepressor expression is incompatible with T(3)-dependent TRH regulation *Endocrinology* 2001; 142: 5321-5331.

16. **Boutell JM, Thomas P, Neal JW, Weston VJ, Duce J, Harper PS, Jones AL**. Aberrant interactions of transcriptional repressor proteins with the Huntington's disease gene product, huntingtin *Human Molecular Genetics* 1999; 8: 1647-1655.

17. **Berghagen H, Ragnhildstveit E, Krogsrud K, Thuestad G, Apriletti J, Saatcioglu F**. Corepressor SMRT functions as a coactivator for thyroid hormone receptor T3Ralpha from a negative hormone response element *J Biol Chem* 2002; 277: 49517-49522.

18. **Berrevoets CA, Umar A, Trapman J, Brinkmann AO**. Differential modulation of androgen receptor transcriptional activity by the nuclear receptor co-repressor (N-CoR) *Biochem J* 2004; 379: 731-738.

19. **Jepsen K, Hermanson O, Onami TM, Gleiberman AS, Lunyak V, McEvilly RJ, Kurokawa R, Kumar V, Liu F, Seto E, Hedrick SM, Mandel G, Glass CK, Rose DW, Rosenfeld MG**. Combinatorial roles of the nuclear receptor corepressor in transcription and development *Cell* 2000; 102: 753-763.

20. **Ahima R, Krozowski Z, Harlan R**. Type I corticosteroid receptor-like immunoreactivity in the rat CNS: distribution and regulation by corticosteroids *J Comp Neurol* 1991; 313: 522-538.

21. **Ahima RS, Harlan RE**. Charting of type II glucocorticoid receptor-like immunoreactivity in the rat central nervous system *Neuroscience* 1990; 39: 579-604.

22. **Van Eekelen JA, Jiang W, de Kloet ER, Bohn MC**. Distribution of the mineralocorticoid and the glucocorticoid receptor mRNAs in the rat hippocampus *J Neurosci Res* 1988; 21: 88-94.

23. **de Kloet ER, Vreugdenhil E, Oitzl MS, Joels M**. Brain corticosteroid receptor balance in health and disease *Endocrine Reviews* 1998; 19: 269-301.

24. **de Kloet ER, Joels M, Holsboer F**. Stress and the brain: from adaptation to disease *Nat Rev Neurosci* 2005.

25. **Beyer HS, Matta SG, Sharp BM**. Regulation of the Messenger Ribonucleic-Acid for Corticotropin-Releasing Factor in the Paraventricular Nucleus and Other Brain Sites of the Rat *Endocrinology* 1988; 123: 2117-2122.

26. **Makino S, Gold PW, Schulkin J**. Corticosterone Effects on Corticotropin-Releasing Hormone Messenger-Rna in the Central Nucleus of the Amygdala and the Parvocellular Region of the Paraventricular Nucleus of the Hypothalamus *Brain Research* 1994; 640: 105-112.

27. **Featherby T, Lawrence AJ**. Chronic cold stress regulates ascending noradrenergic pathways *Neuroscience* 2004; 127: 949-960.

28. **Makino S, Smith MA, Gold PW**. Regulatory role of glucocorticoids and glucocorticoid receptor mRNA levels on tyrosine hydroxylase gene expression in the locus coeruleus during repeated immobilization stress *Brain Research* 2002; 943: 216-223.

29. **Ziegler DR, Cass WA, Herman JP**. Excitatory influence of the locus coeruleus in hypothalamic-pituitary-adrenocortical axis responses to stress *Journal of Neuroendocrinology* 1999; 11: 361-369.

30. **Hagerty T, Fernandez E, Lynch K, Wang SS, Morgan WW, Strong R**. Interaction of a glucocorticoid-responsive element with regulatory sequences in the promoter region of the mouse tyrosine hydroxylase gene *Journal of Neurochemistry* 2001; 78: 1379-1388.

31. **Hagerty T, Morgan WW, Elango N, Strong R**. Identification of a glucocorticoid-responsive element in the promoter region of the mouse tyrosine hydroxylase gene *Journal of Neurochemistry* 2001; 76: 825-834.

32. **Stern CD**. Initial patterning of the central nervous system: how many organizers? *Nat Rev Neurosci* 2001; 2: 92-98.